Overview of Three-Stage Power Converter Topologies for Medium Frequency-Based Railway Vehicle Traction Systems

Athanasios Iraklis, Toni Schirmer, Holger Dittus, Anna Lusiewicz, and Joachim Winter

***Abstract*—With new developments in power electronics and semiconductor devices, there has been an increasing interest in the adoption of power electronic traction transformer (PETT) topologies in railways, mainly for the purpose of mass and volume reduction against conventional topologies. Apart from traction transformers, examples include isolation circuits for on-board auxiliary power units (APU) and even 750 V_{DC}, 110 V_{DC} and lower voltage (e.g., 72 V_{DC}) battery chargers. Special attention has been given to the more mature technology of three-stage (ac–dc–MFac–dc) configurations with intermediate medium frequency ac (MFac) links. In contrast to conventional architectures, it becomes difficult to select a suitable multistage topology of power electronics for the design of complex traction systems with advanced requirements. The power electronics utilized in different configurations have a significant effect on performance, efficiency, power quality (harmonics and stability), and cost indicators for the whole system, making the selection and design process more complex. The objective of this paper is to provide a clear overview of proposed topologies with special emphasis on the power electronic architectures utilized in three-stage PETT systems particularly for railway traction systems and on-board APUs. With regards to the listed range of possible architectures provided to the reader, key characteristics, such as total semiconductor (switches and diodes) count numbers per module per phase, input/output voltage levels, operating frequencies, and the most commonly used resonant networks, are summarized and discussed.**

***Index Terms*—Power electronics, medium frequency transformer, multi-stage converter, railway traction system.**

I. Introduction

CURRENTLY, there is a huge demand for advanced railway traction systems with increased reliability and safety characteristics [1]. In addition, from a technical point-of-view, significant problems, such as high current distortion (harmonics), low power factors and unbalanced voltages and currents in traction-side single-phase AC and DC power supplies require innovative solutions [2]. The utilization of Power Electronics-based Traction Transformer (PETT) setups for railway traction systems using Medium Frequency Transformer (MFT) technologies and Wireless Power Transfer (WPT)-based power supplies, such as in [3], is highly considered for future railway traction systems [4]. The introduction of such advanced systems has the potential to increase design flexibility, system controllability, efficiency and reliability, and to help in the inclusion of other powering solutions, such as on-board and wayside Energy Storage Systems (ESS) as well as recuperating substations [5]. Especially, WPT systems have already revealed advantages in public transportation, such as elimination of range anxiety and reduction of battery size for battery-electric vehicles [6] and, in addition, increased system reliability under extreme weather conditions [7].

A PETT configuration is a system that can be designed to be used in both AC and DC railway distribution networks, with the main aims being the voltage transformation under medium frequency operation, galvanic isolation and reduction of weight and size due to the utilization of higher frequencies (thousands of Hz) [8]. In addition, other features, such as increased modularity, reliability and additional controllability, including power and voltage regulation, voltage sag protection, fault isolation and, depending on the topology, additional useful DC-links [9], are added. Regarding transformation, an MFT-based system can replace the traditional Low Frequency Transformers (LFT) to improve the intelligence level of a railway electrification network, and in addition, it can provide transmission and transformation capabilities between multiple sources and multiple loads [10]. PETT configurations can also accommodate the use of on-board and wayside ESS and boost controllability and energy management features in railway networks, by utilizing the smart railway grid [11] for a more reliable, efficient and modernized power system, or by adopting opportunity-charging techniques for low-cost and emission-free expansion of railway networks [12]. Also, a combination of the afore-mentioned methods has the potential to optimize capturing of regenerative braking energy during braking/downhill operational modes of vehicles in railway micro-grids [13], and thus, reduce energy usage and costs for vehicle operators.

For advanced train designs, such as the Next Generation Train (NGT) HST [14], [15], LINK [16], [17] and CARGO [18] vehicle concepts proposed by the German Aerospace Center (DLR), there are certain design requirements that need to be taken into account, regarding the design of power electronics

Manuscript received February 28, 2018; revised July 21, 2018 and October 21, 2018; accepted December 27, 2018. Date of publication January 25, 2019; date of current version April 16, 2019. The review of this paper was coordinated by Guest editors for Special Section on Smart Rail Mobility. *(Corresponding author: Athanasios Iraklis.)*

A. Iraklis, T. Schirmer, H. Dittus, and J. Winter are with the German Aerospace Center (DLR), Institute of Vehicle Concepts, Stuttgart 70569, Germany (e-mail: athanasios.iraklis@outlook.com; toni.schirmer@dlr.de; holger.dittus@dlr.de; joachim.winter@dlr.de).

A. Lusiewicz is with the University of Stuttgart, Institute of Electrical Energy Conversion, Stuttgart 70569, Germany (e-mail: anna.lusiewicz@iew.uni-stuttgart.de).

Digital Object Identifier 10.1109/TVT.2019.2895500

and isolation stages of a PETT-based power supply. In such advanced systems the selection of a suitable three-stage power electronic conversion architecture, which can provide the electrical interface and galvanic isolation between multiple sources and loads in a distributed way becomes a challenge.

Existing literature review studies have presented broad overviews of proposed PETT systems, with brief descriptions of both three-stage and two-stage topology examples, such as in [19]. Others have focused on different topologies and controls but for electrical distribution applications (both utility and railway supply), such as in [20]. The purpose of this paper is to provide the reader with a clear overview of PETT topologies with focus on the more mature three-stage technology, with configurations that can be used particularly in railway traction systems. Special emphasis is put on the utilized power electronic architectures and their main technical features. Therefore, this overview presents useful examples from literature with focus on the power electronic setups, provides a comparison of different three-stage designs that have been proposed for real-world railway applications and points out the main technical characteristics which should be taken under consideration in design studies.

In Section II, three-stage (AC-DC-MFAC-DC) topology examples are presented. A short description for each of the different setups is given and their main functional and operational characteristics are presented, as given in literature. In Section III, a summary of semiconductor (switches and diodes) count numbers per module per phase, input/output voltage levels and operating frequency values is given for 23 of the discussed setups along with a closing discussion and a brief summary on the most widely utilized resonant topologies for the galvanic isolation stage. A final conclusion is given in Section IV.

II. Overview of Three-Stage PETT-Based Topologies

The three-stage configurations comprise an AC-DC conversion stage (rectification stage), a DC-MFAC conversion stage having a harmonic filter on the converter's primary-side DC-link, an MFAC isolation stage with primary and secondary windings and a final MFAC-DC stage that provides the secondary side DC-link. Three-stage PETT-based converter topologies are otherwise called Isolated Back End (IBE) converters, as in [21]. With regards to the isolation stage, Single-Winding (S-W), Multi-Winding (M-W), Multi-Separated Winding (MSW) and Three-Phase-Winding (3PH-W) topologies have been considered.

In this paper, the developments include three-stage circuitry suggestions after the introduction of silicon-based Insulated Gate Bipolar Transistors (IGBT). For the sake of presenting fully controlled configurations, previous developments based on partially controlled Gate Turn-Off (GTO) thyristors [22] are not considered. Cascaded and non-cascaded DC-MFAC-DC converter topologies (e.g., for Auxiliary Power Units (APU) such as in [23] or battery chargers) are included, as an additional AC-DC conversion stage (input stage) will be required in any case for both single- or multi-phase AC traction systems. The intermediate MFAC-link is sometimes given in literature as HFAC (i.e., High Frequency Alternating Current), as in [24], but in this paper, the term MFAC will be used in order to avoid confusion between kHz- and MHz-level transformation.

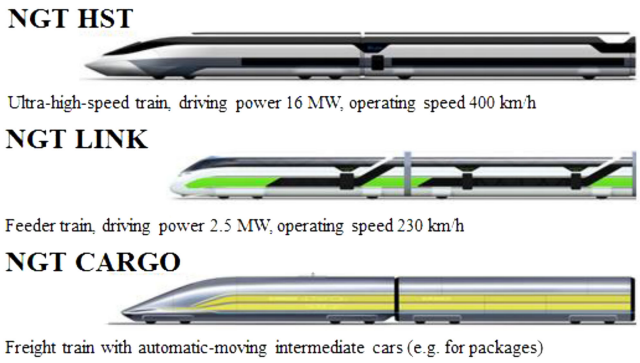

Fig. 1. Next Generation Train (NGT) HST, LINK, and CARGO vehicle concepts proposed by the German Aerospace Center (DLR).

Cascaded three-stage configurations have been widely proposed for MFT- and WPT-based railway traction systems. They are the most common to find in existing setups due to the flexibility the additional input AC-DC rectification stage and primary-side DC-link offer. They feature a DC-MFAC-DC stage for full isolation between the primary- and secondary-side DC-links [25] and capability for reactive power regulation [8]. Additional AC-DC input rectifiers and DC-AC output load inverters are included for the power supply- and load-side AC-links respectively.

Having similar topology requirements to MFTs, the WPT system introduces contactless energy transfer between primary and secondary windings of an air-gap-based MFT, and it is expected to bring several advantages compared to existing railway traction systems [26]. It has a strong potential to solve energy supply-related problems in railways, such as high wear on pantographs and unstable power supply due to conditions where contact between the pantograph and the catenary is lost at high travelling speeds [27]. Examples of WPT for railway applications include static charging when a battery-electric railway vehicle arrives at stations, such as in [28] and dynamic WPT, such as in [29], with the Inductive Power Transfer (IPT) system being considered for practical applications so far [30], [31]. As an example for WPT, the high-level schematic for an IPT-based traction system concept proposed by DLR within the NGT project can be found in [32].

For reference, high-level schematic of MFT-based traction system examples are shown in Fig. 2, Fig. 3 and Fig. 4, as in [33]. With regards to the figures, the interface of interest for this particular review work is defined by the bounds of the AC power supply (three-phase or single-phase) and the on-board secondary-side DC-link.

A. Cascaded Three-Stage PETT-Based Topologies

In this section, cascaded configurations that use series connections of input modules are discussed. Most of the developments listed here are for single-phase power supply systems, but some three-phase-based systems (mainly for WPT purposes) are also presented. The list includes Full Active Bridge (FAB)-, Half

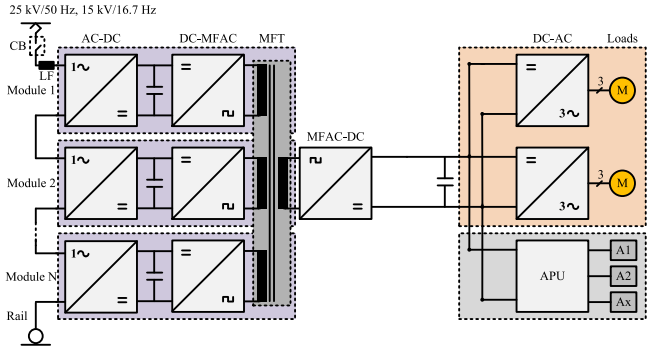

Fig. 2. Example of IBE AC-DC converter topology with cascaded Input-Series-Output-Parallel (ISOP) setup, multi-separated input DC-links, and a M-W isolation setup.

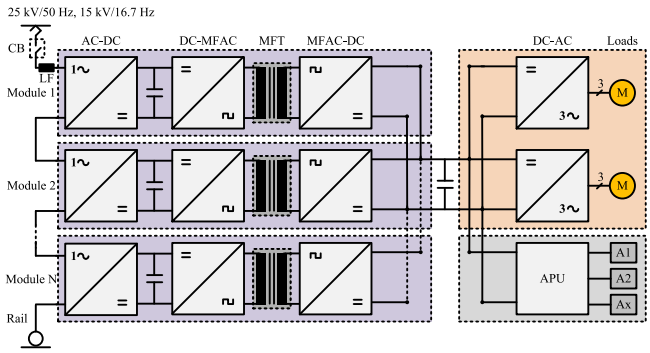

Fig. 3. Example of IBE AC-DC converter topology with cascaded Input-Series-Output-Parallel (ISOP) setup, multi-separated input DC-links, and a MSW isolation setup.

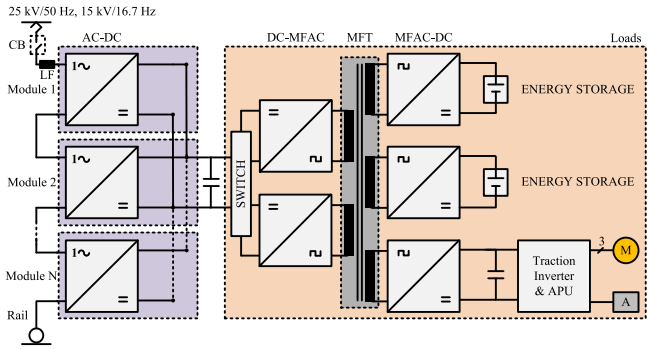

Fig. 4. Example of IBE AC-DC converter topology with a cascaded rectification stage, parallel input DC-links, and a multi-port M-W isolation setup.

Active Bridge (HAB)- and clamping-based (CL) circuitry, including some additional setups.

1) Cascaded Full Bridge-Based Topologies: Back in 1996, a three-stage converter based on cascaded FAB modules on both the primary and secondary sides was proposed by Rufer et al. [22], for single-phase 15 kV_{AC}/16.7 Hz railway traction systems. The input stage of the topology was based on high voltage IGBTs, which had the full controllability advantage over their predecessors; the partially controllable GTO thyristors found in previous developments, such as in [34]. Due to the high catenary operating voltage, the input power modules (active rectifier/inverter units) were connected in series while the outputs of the isolated DC-MFAC-DC stages were connected in parallel,

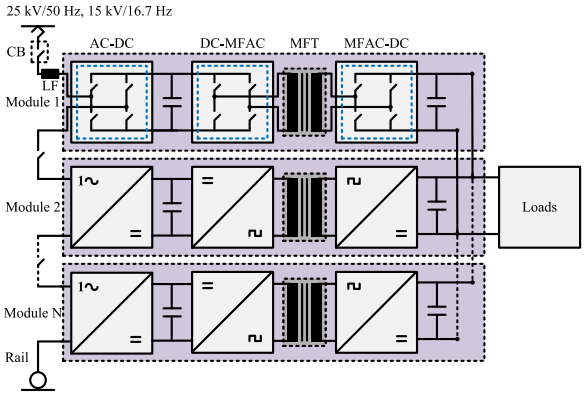

Fig. 5. Single-phase cascaded FAB AC-DC converter topology with MSW isolation and ISOP setup.

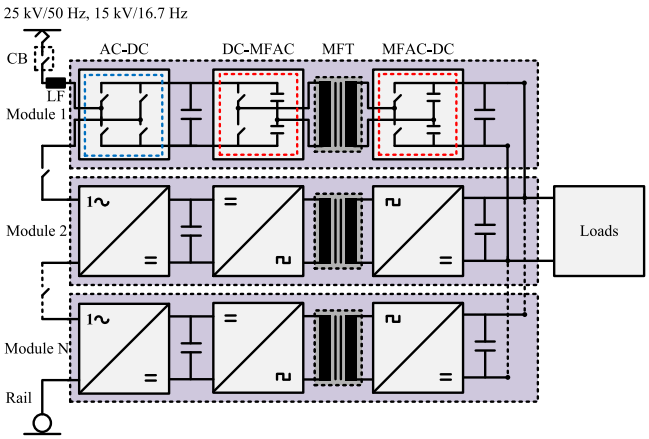

Fig. 6. Single-phase cascaded AC-DC converter topology with a HAB setup on the primary windings.

forming the Input-Series-Output-Parallel (ISOP) configuration [35], which has been very popular in high voltage, high power applications since today [36]. This allowed avoiding the simultaneous switching of series-connected devices, achieving proper sharing of voltage and reactive power and utilizing higher fundamental frequencies (10 kHz) and bidirectional power flow. The isolation stage comprised an MSW setup. The features of this early design were widely used in later developments [37], although the fault-tolerant capability was compromised when an S-W or an M-W isolation stage was used.

In [38], a similar architecture was proposed by Siemens. This FAB-based setup had a holistic ISOP configuration from AC input to DC output and utilized an input switch bank for isolation of modules in case of failure. Moreover, it used Series Resonant Tanks (SRT) [39] in order to avoid hard-switching operation and MSWs. The MSW setup allowed increased reliability in case of module failure and easier manufacturing and installation, as several smaller transformers were easier to be constructed in large numbers. Based on the same concept, in [40], Rufer et al. proposed a three-stage FAB-based re-configurable converter, for use in both 15 kV_{AC}/16.7 Hz and 3 kV_{DC} traction systems, which, compared to conventional LFTs of that time, showed more than 5% less losses when 8 kHz isolation transformers were considered. The converter was able to cope with both AC and DC traction systems via the utilization of a switch box

on the input stage, which allowed increased system flexibility in cases where different traction systems had to be utilized, such as in multi-current locomotives. In [41] and [42], a FAB-based PETT system was proposed, consisting of two active FAB rectifiers/inverters connected in series and two Voltage-Source Converters (VSC) on the primary side, a 2:1 isolation transformer with a M-W coil setup and a FAB voltage-source rectifier/inverter on the secondary side for bidirectional power flow. The disadvantage of this configuration was that, due to the small number of input modules and the M-W coil setup, the converter lacked redundancy in case of module failure.

In [43], [44] and [45], the two FAB-based PETT traction systems had the same front-end setup and SRTs, but different isolation and output stages. The one suggested for electric multiple units had a M-W isolation transformer setup, while the second, which was suggested for locomotives, had MSWs. The new feature in both configurations was the multi-port output configuration. For a single-phase catenary connection of 25 kV_{AC}/50 Hz, the topologies used 23 modules and a switching frequency of 20 kHz. With FAB-based system being the most popular, similar configurations were presented in [46] and [47], for practical single-phase-based applications. For example, in [46], a PETT-based topology was presented by Bombardier for a 15 kV_{AC}/16.7 Hz catenary system, especially for Germany, Austria, Switzerland and the Scandinavian countries, where this particular system is the main type in railway networks [48]. To achieve the high catenary voltage of 15 kV_{AC} and include some redundancy for the system, 8 sub-systems were connected in series at the input-side, each utilizing 6.5 kV_{BV} IGBTs for a DC-link voltage of 3.6 kV_{DC}. The outputs of the secondary-side four-quadrant converters were connected in parallel and the system achieved soft-switching operation for all switching elements, which allowed switching frequencies up to 10 kHz with SRTs. A transformer ratio of 1:1 allowed the use of the same IGBTs for the primary and secondary side DC-links. FAB-based topologies have been utilized also for early dynamic IPT systems, such as the one presented by the Korea Railroad Research Institute (KRRI) in [49], which was IGBT-based, operated at 60 kHz, and utilized series-series compensation and a transformation ratio of 5:8 for a nominal 2.8 kV_{DC} secondary DC-link voltage.

2) Cascaded Half Bridge-Based Topologies: The PETT-based system proposed by ABB in [50]–[53] employs a cascaded HAB-based configuration on the DC-MFAC-DC stage, which has the potential of having reduced system costs, due to the smaller number of switching elements used in the setup. The configuration consisted of 9 modules (following the N+1 rule for redundancy), each rated at only a fraction of the maximum power, in a holistic ISOP setup, and included a main circuit breaker, an input choke and a start-up circuit on the AC side. The number of modules was selected also with regards to line over-voltage, second harmonic ripple in the DC-link voltages and the control strategy [52]. 6.5 kV_{BV} IGBTs were used to meet the high catenary voltage of 15 kV_{AC}/16.7 Hz and the primary 3.6 kV_{DC} DC-link, and 3.3 kV_{BV} IGBTs were used on the 1.5 kV_{DC} DC-link of the secondary side. By employing LLC resonant tanks on the primary sides of the isolation stages, the system showed a maximum efficiency of around 96% due to Zero Voltage Switching (ZVS) turn-on and low-current turn-off conditions for the switches, and Zero Current Switching (ZCS) conditions for the secondary side diode rectifiers. In addition, low harmonic content on the input side and almost a unity power factor for the whole output power range was presented [54].

In [55], a slightly different cascaded ISOP configuration with modular HAB-based Dual Active Bridge (DAB) isolated converters was presented. This setup utilized Phase-Shift Modulation (PSM), bidirectional power flow with a half bridge on the primary windings and low switching losses due to the achievement of ZVS operation for all switching devices. A low-power experimental setup had a switching frequency of 50 kHz and 4 switching elements per module for the DC-MFAC-DC conversion and achieved up to 97% of efficiency for a wide load range. In this configuration, an adaptive inductor was introduced as the main energy transfer element so that the circulating energy could be optimized for ZVS operation at low load conditions and increased efficiency at high load conditions.

3) Other Cascaded Three-Stage Topologies: In [56], a cascaded diode-clamped three-stage PETT-based system with MSW transformers and a holistic ISOP setup was proposed for a 25 kV_{AC}/50 Hz railway traction system. Each module comprised a FAB rectifier and a HAB bidirectional DC-MFAC inverter with clamped diodes on the primary side, and a HAB bidirectional MFAC-DC rectifier with clamped diodes on the secondary side. However, it was pointed out that, at that time, FAB-based designs could reach higher voltage and power levels as they were more mature than diode-clamped converters [57]. The challenges for the latter were the unbalanced voltages and increased switching losses.

In [58], a hybrid Metal-Oxide Semiconductor Field-Effect Transistor (MOSFET)-IGBT modified multi-level topology was proposed for an IPT system, with the aim of reducing the number of components and conduction losses. It used a modified multi-level MOSFET converter and an IGBT-based FAB converter on the primary side of the isolation stage. The modified multi-level stages consisted of series connected half bridge converters and individual voltage-level sources. Compared to its predecessor [59], the proposed topology utilized a lower number of switches, similarly to [60]. In [61], a cascaded DC-DC converter based on series connections of 1.5 kV_{BV} Silicon Carbide (SiC)-based Junction Gate Field-Effect Transistors (JFET) and low voltage silicon MOSFETs on the input side and fast 0.6 kV_{BV} IGBT switches on the output side was presented. A bidirectional DAB configuration was used on 5 kV_{DC} input and 700 V_{DC} output DC-links. The isolation transformer operated with a frequency of 50 kHz. The low-voltage MOSFETs were used to control the behavior of the JFETs, as the series connection resulted in a normally off behavior although the JFETs are normally off devices. The 1.5 kV_{BV} JFETs were used to block the 5 kV_{DC} input DC-bus voltage and the on/off states of all the switches were simply controlled via the MOSFET's gate; no special drivers were required. Due to a $\pi/3$ PSM, all switches could operate under ZVS conditions, so no turn on losses could occur. It was demonstrated that the configuration had negligible turn-off losses; turn-off losses are relevant for the phase-shift operation of the DAB topology. That was due to the fact that

turn-off energy was independent of the current due to the existence of parasitic capacitances on the switches (where energy is stored).

B. Non-Cascaded Three-Stage PETT-Based Topologies

This section lists non-cascaded three-stage configurations, basically DC-MFAC-DC conversion systems for DC input power supplies. Such configurations can be found, for example, in pure tram or train-tram setups where DC overhead catenaries are used [62] or in DC-link-connected APUs and battery chargers that require isolation between the input and the output sides [63]. The list includes configurations based on the same categories of the previous cascaded three-stage topologies section.

1) Non-Cascaded Full Bridge-Based Topologies: In [64], a non-cascaded PETT-based system was presented in two versions. The first utilized a DAB converter with a 1 kHz S-W silicon-based transformer, while the second one used a Series Resonant Converter (SRC) for higher power density [65], [66], which evolved into an LLC resonant converter for ZCS operation of the IGBT switches, with a 5 kHz S-W nano-crystalline transformer. Both configurations used 6.5 kV_{BV} IGBTs on the 3 kV_{DC} primary DC-link, while 1.7 kV_{BV} IGBTs were used on the secondary DC-link with the isolation transformer having a transformation ratio of 4:1. The system achieved rated efficiency values of more than 99%.

For the design presented in [67], [68] by Bombardier, a resonant inverter was presented for powering of linear induction motors used in urban transit applications. The configuration allowed soft-switching operation of the primary-side IGBTs, which allowed high switching frequencies and lower losses. The choice for a resonant converter was due to the fact that, unlike Pulse Width Modulation (PWM)-based converters, resonance provided the advantage of operating at higher frequencies with reduced Electro-Magnetic Interference (EMI) levels. Within the design and test parameters, a switching frequency of 25 kHz was used. The setup showed efficiency values between 94.9% for 5% load and 99% for full load on 750 V_{DC}. For an input voltage of 600 V_{DC} (worst case scenario for voltage drops) the recorded efficiency was 85.6% for full load. On the other hand, the DAB topology presented in [69] with the two active bridges allowed bidirectional power flow, simple voltage and power regulation with both step-down and step-up operation. In this publication, non-dissipative snubbers were also proposed for DAB converters. However, in the DAB configuration, the efficiency depends on the converter input/output voltage levels and they are suitable only in certain applications. In SRCs, and especially in dual-active SRC configurations [70], no snubbers are required due to the use of low turn-off currents. However, in this topology, the efficiency strongly depends on the resonant frequency and the dead-times.

2) Non-Cascaded Half Bridge-Based Topologies: In [71], a Single Active Bridge (SAB) resonant converter with a half-bridge configuration with only two transistors, a series resonant circuit on the primary side and a Full Passive Bridge (FPB) rectifier on the secondary side was proposed for 3 kV_{DC} and 600 V_{DC} DC tram-train systems. The prototype utilized 6.5 kV_{BV} IGBTs and a nano-crystalline transformer designed for soft-switching conditions up to 2.7 kHz, in contrast to the 300 Hz to 400 Hz range used at that time for hard-switching operation. The main disadvantages of the system were the narrow range of adjustment, the additional power capacitors and power chokes required and the non-bidirectional power flow. On the other hand, the SAB converter introduced in [72] was a simple solution for high power applications where power or voltage regulation was not required. At that time, the use of capacitive snubbers on the primary side of SAB topologies was widely extended with the goal of reducing semiconductor turn-off losses. In [73], a 100 kVA auxiliary power supply developed by Bombardier Transportation in 1996/1997 using a PETT-based configuration with a Two-Quadrant Converter (2QC) on the input side was presented. The topology was designed for 5 different input voltages (including 3 kV_{AC}), with 6 input converter modules (1 for redundancy) utilizing 1.7 kV_{BV} IGBTs and a switch box on the input-side, which was used for the realization of the different configurations for the different voltage inputs. From a cost point-of-view, the increase in the number of components was compensated through the lower costs of the low voltage (and low power) inverters on the secondary side. The configuration was also suggested for cascaded holistic ISOP setups.

3) Other Non-Cascaded Three-Stage Topologies: In [74], isolated multi-phase SAB, DAB and SRC topologies were presented. A case study utilized 20 kHz as the switching frequency and a transformation ratio of 1:1. In [75], a soft-switching converter with an active clamp circuit and dual resonant structures was presented for low power applications. The dual resonant tanks of the leakage inductors and the resonant capacitors were used to achieve ZCS turn-off operation of the secondary side diodes. By using an asymmetrical PWM scheme, the active clamp circuit created ZVS turn-on operation for all switches. The topology achieved a constant switching frequency of 90 kHz, resonant frequencies of 139 kHz for the primary and 126 kHz for the secondary sides respectively and peak efficiency of 93%. The topology was compared to a half bridge resonant converter proposed by Kim et al. [76] with similar characteristics but with variable switching frequency, a single switch isolated converter proposed by Park et al. [77] which could not provide ZVS operation for switches nor ZCS operation for diodes, an active clamp forward converter proposed by Kim et al. [78], a phase shift full bridge converter proposed by Park et al. [79] and a phase shift full bridge converter proposed by Yoon et al. [80], which only offered ZVS operation for switches.

III. Discussion

A. Summary of Discussed Three-Stage PETT-Based systems

In this section, main technical aspects of 23 of the discussed AC-DC converter topologies are summarized. Table I presents the setups used for each stage, total semiconductor count numbers per module per phase, input/output voltage levels and operating frequencies for three-stage PETT-based configurations in chronological order.

PETT architectures can reduce the energy usage of railway vehicles due to their increased efficiency characteristics and

TABLE I
TECHNICAL SUMMARY OF THREE-STAGE PETT-BASED TOPOLOGIES

Publication	1st stage	2nd stage	Isolation	3rd stage	Semiconductors per mod.phase	Voltage Rating	Operating Frequency
[69] 1992	X	$FAB_{(4)}$	S-W/M-W	$FAB_{(4)}/HAB_{(2)}$	$X+4_{(P)}$, $4/2_{(S)}$	200 V_{DC} to 1.6 kV_{DC}	50 kHz
[22] 1996	$FAB_{(4)}$	$FAB_{(4)}$	MSW	$FAB_{(4)}$	$12_{(P+S)}$	15 $kV_{AC(input\ AC\text{-}link)}$	10 kHz
[73] 2001	$2QC_{(5D+1)}$	$HAB_{(2)}$	MSW SRT	$FPB_{(4D)}$	$3+9D_{(P+S)}$	3 kV_{AC} to 1.5 kV_{DC}	10 kHz
[47] 2002	$FAB_{(4)}$	$FAB_{(4)}$	MSW SRT	$FAB_{(4)}$	$12_{(P+S)}$	15 kV_{AC} to 3 kV_{DC}	10 kHz
[40] 2003	$FAB_{(4)}$	$FAB_{(4)}$	MSW	$FAB_{(4)}$	$12_{(P+S)}$	15 kV_{AC} and 3 kV_{DC}	8 kHz
[72] 2005	X	$HAB_{(2)}$	S-W	$FPB_{(4D)}$	$X+2+4D_{(P+S)}$	LV_{AC} to 400 V_{DC}	10 kHz
[46] 2007	$FAB_{(4)}$	$FAB_{(4)}$	MSW SRT	$FAB_{(4)}$	$12_{(P+S)}$	15 kV_{AC} to 3.6 kV_{DC}	8 kHz
[77] 2007	X	$CL_{(1+1D)}$	S-W Res.	$PR_{(2D)}$	$X+1+3D_{(P+S)}$	100 V_{DC} to 48 V_{DC}	42 kHz
[42] 2008	$FAB_{(4)}$	$FAB_{(4)}$	M-W	$FAB_{(4)}$	$8_{(P)}$, $4_{(S)}$	600 $V_{DC(output\ DC\text{-}link)}$	0.4 kHz
[61] 2008	X	$FAB_{(4)}$	S-W	CL $FAB_{(8+4D)}$	$X+4_{(P)}$, $8+4D_{(S)}$	5 kV_{DC} to 700 V_{DC}	50 kHz
[67] 2010	X	$FAB_{(4)}$	S-W LLC	$PR_{(2D)}$	$X+4+2D_{(P+S)}$	750 V_{DC} to 700 V_{AC}	25 kHz
[75] 2010	X	$CL_{(2)}$	S-W Res.	$PR_{(2D)}$	$X+2+2D_{(P+S)}$	380 V_{DC} to 190 V_{DC}	90 kHz
[55] 2011	$FAB_{(4)}$	$HAB_{(2)}$	MSW	$HAB_{(2)}$	$8_{(P+S)}$	7.2 kV_{AC} to 400 V_{DC}	50 kHz
[52] 2012	$FAB_{(4)}$	$HAB_{(2)}$	MSW LLC	$HAB_{(2)}$	$8_{(P+S)}$	15 kV_{AC} to 1.5 kV_{DC}	1.5 kHz
[64] 2012	X	$FAB_{(4)}$	S-W SRT	$FAB_{(4)}$	$8_{(P+S)}$	3 kV_{DC} to 750 V_{DC}	5 kHz
[59] 2014	X	$FAB_{(4)}$	S-W LCC	$FAB_{(4)}$	$X+4_{(P)}$, $4_{(S)}$	600 V_{DC} to 300 V_{DC}	70 kHz
[58] 2014	X	$HAB_{(2)}+FAB_{(4)}$	S-W LCC	$FAB_{(4)}$	$X+2_{(Boost)}$, $8_{(P+S)}$	600 V_{DC} to 300 V_{DC}	80 kHz
[71] 2014	X	$HAB_{(2)}$	S-W SRT	$FPB_{(4D)}$	$X+2+4D_{(P+S)}$	3 kV_{DC} to 600 V_{DC}	2.7 kHz
[43] 2015	$FAB/FPB_{(4)}$	$FAB_{(4)}/HAB_{(2)}$	M-W/MSW LLC	$FAB_{(4)}/HAB_{(2)}$	$8/2+4D_{(P)}$, $4/2_{(S)}$	25 kV_{AC} to 1.8 kV_{DC}	20 kHz
[49] 2015	3PH $FAB_{(2)}$	$FAB_{(4)}$	MSW SRT	$FPB_{(4)}$	$2_{(R)}$, $4_{(P)}$, $4_{(S)}$	400 V_{AC} to 2.8 kV_{DC}	60 kHz
[56] 2015	CL $FAB_{(8+4D)}$	CL $HAB_{(4+2D)}$	MSW	CL $HAB_{(4+2D)}$	$16+8D_{(P+S)}$	25 kV_{AC} to 2 kV_{DC}	3 kHz
[8] 2017	X	3PH $M^2LC_{(12)}$	3PH-W	3PH $FAB_{(4)}$	$X+4_{(P)}$, $2_{(S)}$	10 kV_{AC} to 700 V_{DC}	20 kHz
[74] 2017	X	3PH $FAB_{(6)}$	3PH-W	3PH $FPB_{(6D)}$/3PH $FAB_{(6)}$	$X+4/2+2D_{(P+S)}$	500 V_{DC} to 500 V_{DC}	20 kHz

X: Not Defined, Res.: Resonant Tank, R: 3-Phase Primary Rectifier, P: Primary Side, S: Secondary Side, Boost: Boost Converter, D: Diode

lower mass, compared to conventional low-efficiency, heavy-weight LFTs [32] (especially the LFTs designed for 16.7 Hz operation), resulting in lower operational costs. This is accomplished via the utilization of low-resistance switching elements and higher switching frequencies, as in Table I, which allows for higher power densities with reduced copper and magnetic material requirements for the galvanic isolation stage. Cooling requirements are also likely to be reduced via the utilization of low-resistance switching devices exhibiting lower junction temperature rise [19] and via the use of resonance-based control techniques, as discussed in the next section, for the reduction of switching losses. From a system point-of-view, this further reduces energy usage and associated costs. Reduced weight and size can also have a positive impact on mechanical wear of wheel and rail contact surfaces and passenger capacity respectively, possibly resulting in lower maintenance costs and increased income for operators. Especially for EMUs, the space under the floor for integrating the main transformer is very limited. For decentralized traction, high power density becomes an advantage of PETT systems for advanced traction.

However, the utilization of very high switching frequencies (>50 kHz) at high voltage and current levels is strongly limited by semiconductor characteristics, such as turn-on/turn-off times, junction-to-case heat dissipation and blocking voltages. As seen in most of the listed examples, more complex cascaded structures mainly based on FAB converters with lower-rating advanced fast semiconductor elements solve this problem, but reliability becomes an issue due to increased component count, as illustrated in Table I. That requires the adoption of effective fault-tolerant control methods [81] along with highly desirable advanced condition monitoring techniques [82] that further increase the system's complexity and initial design and investment costs. Setups based on HAB converters have lower component count but exhibit lower power ratings due to semiconductor current limitation and the requirement of high-frequency capacitor legs. The necessity of advanced gate driver units and the utilization of expensive soft magnetic cores also add to the initial investment.

On the other hand, modularity reduces voltage and current stresses for the semiconductors, which boosts the lifetime of switching elements. It is also possible to have increased online redundancy with easily-scalable spare modules for live maintenance purposes [83]; individual cascaded modules may be switched off if an irreversible fault is developed. Multi-system operation adds to the advantages of PETT systems as an increased flexibility feature. In order to reduce the cost of a PETT system, it becomes necessary to optimize the number of

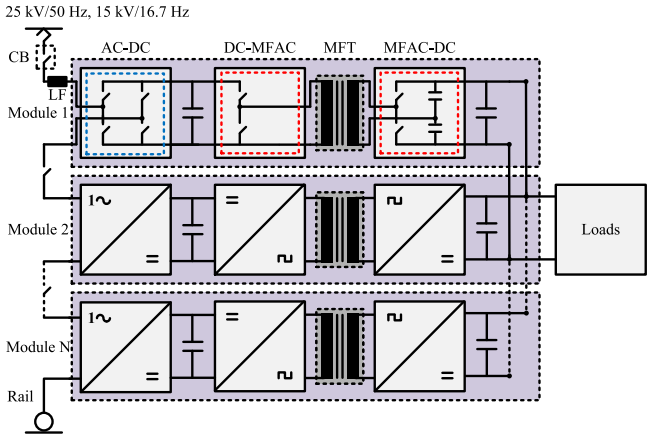

Fig. 7. Single-phase cascaded AC-DC converter topology with an asymmetrical HAB setup on the primary windings.

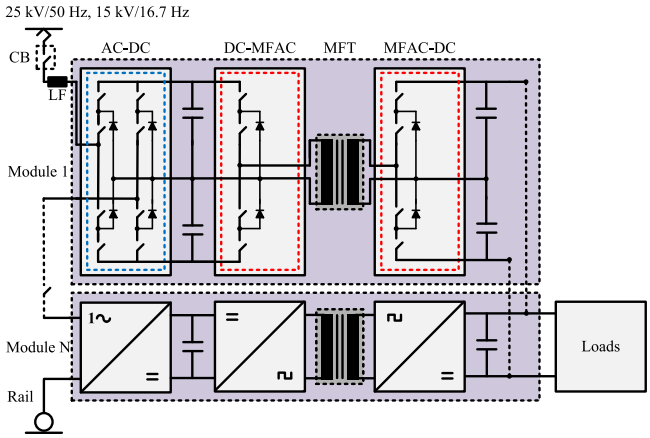

Fig. 8. Single-phase cascaded diode-clamped AC-DC converter topology with half-bridges on the primary and secondary windings.

cascaded modules for minimized component count and optimize the design of the isolation stage in order to minimize the use of expensive copper and soft magnetic core materials. As the component count becomes a key factor, the utilization of two-stage (AC-MFAC-DC) architectures with no intermediate DC-link on the primary side has the potential to result in lower cost and increased efficiency and reliability due to the smaller number of conversion stages required [84]. As in [21], two-stage converter topologies are otherwise called Isolated Front End (IFE) converters. An example of a cascaded IFE converter with an MSW isolation stage is given in Figure 7.

B. Resonant Circuits in the Galvanic Isolation Stage

In order to achieve soft-switching operation with reduced switching losses for the power semiconductors, a variety of resonant circuit configurations for the isolation stage has been proposed. As it can be seen from the listed proposed architectures, most of the setups have utilized resonant tanks in the isolation stage, especially the ones having relatively increased switching frequencies. Resonance-based setups offers better soft-switching characteristics (especially during turn-off) with lower power losses, which are necessary for properly

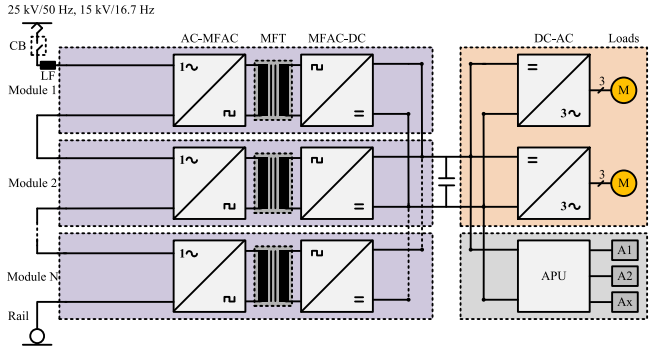

Fig. 9. Example of IFE AC-DC converter topology with a cascaded Input-Series-Output-Parallel (ISOP) setup and a MSW isolation stage.

controlling heat dissipation, and case and junction temperatures for the power modules, and lower EMI emissions. It is also possible to achieve soft-switching conditions (ZVS for primary switches and ZCS for secondary switches and diodes) with phase shifting modulation. However, in those cases, the ZVS region is highly load-dependent, can be limited under low load conditions [85] and high turn-off switching losses due to high turn-off currents usually take place [86]. This section summarizes the most widely adopted resonant topologies founded in SRC, Parallel Resonant Converters (PRC) and Series-Parallel Resonant Converters (SPRC).

In SRCs, the power in the isolation stage can be adjusted via frequency control [87] above resonance [85]; the current delivered to the resonant circuit lags the voltage applied to the resonant circuit. For example, in [88], in order to achieve ZVS operation for the MOSFETs of the full H-bridge converter, the operating frequency is modulated above the resonance frequency. Depending on the design, the minimum duty cycle values define the ZVS range, which sometimes can be limited. With certain control methods, such as the Half Cycle-Discontinuous Conduction Mode (HC-DCM) in [89], [90], it is also possible to achieve load-independent ZVS operation by utilizing the magnetizing current of the isolation stage of an SRC. However, the main disadvantage of SRCs is that proper output voltage control cannot be achieved under no-load conditions. This means the topology can be used in applications that do not require load regulation. Another disadvantage is that the output DC filter might have to carry a high current ripple, depending on the design of the secondary side. This could prevent the use of this particular topology in low-voltage high-current applications. However, this should not be an issue in high-voltage applications. The topology is also considered suitable for high power applications where a full H-bridge converter is selected, as the resonant capacitors act as dc-blocking capacitors [91]. The necessity for additional controls due to unbalanced switching times or forward voltage drops is eliminated.

On the other hand, PRCs are controllable during no-load operation with operating frequency above resonance by using parallel capacitors. However, the current in the semiconductors and the reactive components remains relatively fixed for the whole load range, which results in overall reduced efficiency when load varies. Also, circulating energy is higher, increases as the input DC voltage increases and exists even during

no-load operation. Thus, the converter is considered to be suitable for applications with narrow input DC voltage range and non-varying load close to the rated one. In contrast to SRCs, PRCs are suitable for low-voltage high-current applications, due to the fact that the DC filter on the secondary side is of the inductor input type, which reduces the current ripple.

An SPRC combines the advantages of the SRCs and PRCs together. The topology is able to deal with voltage regulation under no-load conditions and reduce the circulating currents with regards to load. With proper selection of the resonant components, the converter essentially operates as an SRC at high loads and takes on the characteristics of PRCs as the load decreases [91]. The SPRC is also naturally short-circuit-proof [92], which is one of the main characteristics of the PRCs. In addition, due to the higher degree of freedom, it is able to make smart use of the parasitic elements of the transformer [93], i.e., leakage inductance and winding capacitance, which considerably affect the operation, efficiency and reliability characteristics [94]. However, SPRCs may still have the problem of relatively high circulating currents when the converter works away from resonance. Within the same family, the LCC and LLC types are of particular interest. In these setups, ZVS conditions are achieved along with higher efficiency and power density characteristics [95]. They can work with a wide voltage range utilizing only a narrow range of switching frequencies. Such topologies have become very popular in industrial electronics, transportation systems [68] and electrical vehicle battery chargers [96]. Other similar resonant networks such as the LCL, CLL, CLLC and LCLC types have not gained the same attention due to either not offering as many properties as the LCC and LLC ones or requiring more or larger compensation components.

IV. Conclusion

In this overview, three-stage (AC-DC-MFAC-DC) converter topologies for MFT-based railway traction systems were discussed. The list includes SAB-, DAB- and resonance-based circuitry (with half and/or full H-bridges) for three-stage topologies, including DC-MFAC-DC configurations. Several examples from literature were presented with their main characteristics being pointed out. Main technical aspects (semiconductor count numbers, input/output voltage ratings and operational frequencies) were also listed in the last section for 23 of the discussed systems. An overview of the main characteristics of the most widely adopted isolation stage compensation networks was also presented.

Adding to existing literature review studies and with special focus on three-stage power electronic architectures, this overview dived into several examples especially proposed for railway traction systems utilizing a rectification stage, essentially resulting in the existence of primary and secondary DC-links. A comparison of the different architectures was presented and main technical characteristics, which should be taken under consideration in design studies, were pointed out and discussed, providing the reader with a good understanding of the different features of possible three-stage design solutions for PETT-based railway traction systems and APUs.

References

[1] Q. Xu *et al.*, "Analysis and comparison of modular railway power conditioner for high-speed railway traction system," *IEEE Trans. Power Electron.*, vol. 32, no. 8, pp. 6031–6048, Aug. 2017.

[2] Z. Zhang *et al.*, "Reactive power compensation and negative-sequence current suppression system for electrical railways with YNvd-connected balance transformer—Part I: Theoretical analysis," *IEEE Trans. Power Electron.*, vol. 33, no. 1, pp. 272–282, Jan. 2018.

[3] J. Winter, S. Mayer, S. Kaimer, P. Seitz, J. Pagenkopf, and S. Streit, "Inductive power supply for heavy rail vehicles," in *Proc. 3rd Int. Elect. Drives Prod. Conf.*, 2013, pp. 1–9.

[4] B. Fan, Y. Li, K. Wang, Z. Zheng, and L. Xu, "Hierarchical system design and control of an MMC-based power-electronic transformer," *IEEE Trans. Ind. Inform.*, vol. 13, no. 1, pp. 238–247, Feb. 2017.

[5] V. Gelman, "Energy storage that may be too good to be true: Comparison between wayside storage and reversible thyristor controlled rectifiers for heavy rail," *IEEE Veh. Technol. Mag.*, vol. 8, no. 4, pp. 70–80, Dec. 2013.

[6] H. H. Wu, A. Gilchrist, K. Sealy, P. Israelsen, and J. Muhs, "A review on inductive charging for electric vehicles," in *Proc. IEEE Int. Elect. Mach. Drives Conf.*, 2011, pp. 143–147.

[7] S. M. A. Iqbal, D. J. Thrimawithana, U. K. Madawala, and A. Swain, "A bi-directional inductive power transfer system with individually controlled tracks and pick-ups," in *Proc. IEEE ECCE Asia Downunder*, 2013, pp. 1059–1064.

[8] J. Zhang, Z. Wang, and S. Shao, "A three-phase modular multilevel DC–DC converter for power electronic transformer applications," *IEEE J. Emerg. Sel. Topics Power Electron.*, vol. 5, no. 1, pp. 140–150, Mar. 2017.

[9] T. Zhao, G. Wang, S. Bhattacharya, and A. Q. Huang, "Voltage and power balance control for a cascaded H-bridge converter-based solid-state transformer," *IEEE Trans. Power Electron.*, vol. 28, no. 4, pp. 1523–1532, Apr. 2013.

[10] T. Zhou and Y. Xu, "Fault characteristic analysis and simulation of power electronic transformer based on MMC in distribution network," in *Proc. IEEE Int. Conf. Energy Internet*, 2017, pp. 332–337.

[11] I. Sengor, H. C. Kilickiran, H. Akdemir, B. Kekezoglu, O. Erdinc, and J. P. S. Catalão, "Energy management of a smart railway station considering regenerative braking and stochastic behaviour of ESS and PV generation," *IEEE Trans. Sustain. Energy*, vol. 9, no. 3, pp. 1041–1050, Jul. 2018.

[12] A. Iraklis, C. Iraklis, and A. Hoffrichter, "Catenary free battery electric operation with opportunity charging for light rail networks," *Newsletter*, vol. 4, 2017.

[13] Y. Yoshida, H. P. Figueroa, and R. A. Dougal, "Comparison of energy storage configurations in railway microgrids," in *Proc. IEEE Second Int. Conf. DC Microgrids*, 2017, pp. 133–138.

[14] J. Winter, "Novel rail vehicle concepts for a high speed train: The next generation train," in *Proc. 1st Int. Conf. Railway Technol., Res., Develop., Maintenance*, 2012, pp. 314–326.

[15] J. Winter *et al.*, "Fahrdrahtlose energieüber-tragung bei schienenfahrzeugen des vollbahnverkehrs," 2014.

[16] D. Krüger and J. Winter, "NGT Link: Ein Zugkonzept für schnelle doppelstöckige Regionalfahrzeuge," *ZEVrail-Zeitschrift für das gesamte System Bahn*, vol. 141, pp. 442–449, 2017.

[17] D. Krüger and J. Winter, "NGT LINK: A double-deck train concept for rapid inter-regional transportation," in *Eur. Railway Rev.*, vol. 21, pp. 53–55, 2015.

[18] J. Winter, M. Boehm, G. Malzacher, and D. Krueger, "NGT CARGO–Schienengüterverkehr der Zukunft," *Internationales Verkehrswesen*, vol. 69, pp. 82–85, 2017.

[19] D. Ronanki and S. S. Williamson, "Evolution of power converter topologies and technical considerations of power electronic transformer-based rolling stock architectures," *IEEE Trans. Transp. Electrif.*, vol. 4, no. 1, pp. 211–219, Mar. 2018.

[20] A. Dannier and R. Rizzo, "An overview of power electronic transformer: Control strategies and topologies," in *Proc. Int. Symp. Power Electron. Power Electron., Elect. Drives, Automat. Motion*, 2012, pp. 1552–1557.

[21] J. E. Huber, J. Böhler, D. Rothmund, and J. W. Kolar, "Analysis and cell-level experimental verification of a 25 kW all-SiC isolated front end 6.6 kV/400 V AC-DC solid-state transformer," *CPSS Trans. Power Electron. Appl.*, vol. 2, no. 2, pp. 140–148, 2017.

[22] A.-C. Rufer, N. Schibli, and C. Briguet, "A direct coupled 4-quadrant multilevel converter for 16 2/3 Hz traction systems," in *Proc. 6th IEE Conf. Power Electron. Variable Speed Drives*, Nottingham, U.K., Sep. 23–25, 1996, pp. 448–453.

[23] N. H. Baars, J. Everts, H. Huisman, J. L. Duarte, and E. A. Lomonova, "A 80-kW Isolated DC–DC converter for railway applications," *IEEE Trans. Power Electron.*, vol. 30, no. 12, pp. 6639–6647, Dec. 2015.

[24] M. Wang, S. Guo, Q. Huang, W. Yu, and A. Q. Huang, "An isolated bidirectional single-stage DC–AC converter using wide-band-gap devices with a novel carrier-based unipolar modulation technique under synchronous rectification," *IEEE Trans. Power Electron.*, vol. 32, no. 3, pp. 1832–1843, Mar. 2017.

[25] X. She, A. Q. Huang, and R. Burgos, "Review of solid-state transformer technologies and their application in power distribution systems," *IEEE J. Emerg. Sel. Topics Power Electron.*, vol. 1, no. 3, pp. 186–198, Sep. 2013.

[26] K. Hwang, S. Kim, S. Kim, Y. Chun, and S. Ahn, "Design of wireless power transfer system for railway application," *Int. J. Railway*, vol. 5, no. 4, pp. 167–174, 2012.

[27] S. B. Lee, S. Ahn, J. H. Lee, and I. G. Jang, "Optimization of the wireless power transfer system in an electric railway," in *Proc. IEEE Wireless Power Transfer Conf.*, 2014, pp. 158–161.

[28] C.-B. Park, B.-S. Lee, and H.-W. Lee, "Magnetic and thermal characteristics analysis of inductive power transfer module for railway applications," in *Proc. IEEE Veh. Power Propulsion Conf.*, 2012, pp. 576–579.

[29] M. Li, Q. Chen, J. Hou, W. Chen, and X. Ruan, "8-Type contactless transformer applied in railway inductive power transfer system," in *Proc. IEEE Energy Convers. Congr. Expo.*, 2013, pp. 2233–2238.

[30] H. Zhang, Y. Du, L. Shi, and R. Zhang, "Study on a spoon shape magnetic core contactless transformer for the ICPT system in railway transportation," in *Proc. IEEE Transp. Electrif. Conf. Expo*, 2017, pp. 1–6.

[31] P. Seitz, N. Parspour, and M. Zimmer, "A scaled model for investigations of three-phase contactless energy transfer systems," in *Proc. IEEE Wireless Power Transfer Conf.*, 2017, pp. 1–4.

[32] S. Streit and J. Winter, "Contactless energy transfer for main-line rail vehicles," *15. Internationales Stuttgarter Symposium*, Wiesbaden, Germany: Springer, 2015, pp. 1587–1598.

[33] T. Besselmann, A. Mester, and D. Dujic, "Power electronic traction transformer: efficiency improvements under light-load conditions," *IEEE Trans. Power Electron.*, vol. 29, no. 8, pp. 3971–3981, Aug. 2014.

[34] H. Weiss, "Elimination of the 16 2/3 Hz, 15 kV main transformer on electric traction vehicle," in *Proc. 1st Eur. Power Electron. Appl. Conf.*, Brussels, Belgium, 1985, pp. 5.83–5.88.

[35] S. Östlund, "Reduction of transformer rated power and line current harmonics in a primary switched converter system for traction applications," in *Proc. 5th Eur. Conf. Power Electron. Appl.*, Brighton, U.K., 1993, pp. 112–119.

[36] L. Wang, A. Q. Huang, and Q. Zhu, "Multi-objective optimization of medium voltage SiC DC-DC converter based on modular input-series-output-parallel (ISOP) architecture," in *Proc. IEEE 3rd Int. Future Energy Electron. Conf.*, 2017, pp. 627–632.

[37] J. Feng, W. Q. Chu, Z. Zhang, and Z. Q. Zhu, "Power electronic transformer-based railway traction systems: Challenges and opportunities," *IEEE J. Emerg. Sel. Topics Power Electron.*, vol. 5, no. 3, pp. 1237–1253, Sep. 2017.

[38] G. Kratz and H. Strasser, "Drive concepts for future railway vehicles," *Elektrische Bahnen*, vol. 96, no. 11, pp. 333–337, 1998.

[39] I. O. Lee, S. Y. Cho, and G. W. Moon, "Three-level resonant converter with double LLC resonant tanks for high-input-voltage applications," *IEEE Trans. Ind. Electron.*, vol. 59, no. 9, pp. 3450–3463, Sep. 2012.

[40] A. Rufer, N. Schibli, C. Chabert, and C. Zimmermann, "Configurable front-end converters for multicurrent locomotives operated on 16 2/3 Hz AC and 3 kV DC systems," *IEEE Trans. Power Electron.*, vol. 18, no. 5, pp. 1186–1193, Sep. 2003.

[41] T. Komrska and Z. Peroutka, "Main traction converter with medium-frequency transformer: Control of converters around MF transformer," in *Proc. Int. Symp. Power Electron., Elect. Drives, Automat. Motion*, 2008, pp. 1194–1198.

[42] J. Zak and Z. Peroutka, "Laboratory prototype of traction converter with medium-frequency transformer: Master control and diagnostic unit," in *Proc. Int. Symp. Power Electron., Elect. Drives, Automat. Motion*, 2008, pp. 1002–1007.

[43] C. Gu, Z. Zheng, and Y. Li, "A power electronic transformer (PET) with multiport bidirectional resonant DC-DC converters for electric traction applications," in *Proc. IEEE Transp. Electrif. Conf. Expo*, 2015, pp. 1–6.

[44] C. Gu, Z. Zheng, and Y. Li, "Power characteristics of isolation units in a novel power electronic transformer (PET) for locomotive traction applications," in *Proc. 17th Int. Conf. Elect. Mach. Syst.*, 2014, pp. 2779–2784.

[45] C. Gu, Z. Zheng, L. Xu, K. Wang, and Y. Li, "Modeling and control of a multiport power electronic transformer (PET) for electric traction applications," *IEEE Trans. Power Electron.*, vol. 31, no. 2, pp. 915–927, Feb. 2016.

[46] M. Steiner and H. Reinold, "Medium frequency topology in railway applications," in *Proc. Eur. Conf. Power Electron. Appl.*, 2007, pp. 1–10.

[47] L. Heinemann, "An actively cooled high power, high frequency transformer with high insulation capability," in *Proc. 17th Annu. IEEE Appl. Power Electron. Conf. Expo.*, 2002, vol. 1 pp. 352–357.

[48] A. Steimel, "Power-electronic grid supply of AC railway systems," in *Proc. 2012 13th Int. Conf. Optim. Elect. Electron. Equip.*, 2012, pp. 16–25.

[49] J. H. Kim *et al.*, "Development of 1-MW inductive power transfer system for a high-speed train," *IEEE Trans. Ind. Electron.*, vol. 62, no. 10, pp. 6242–6250, Oct. 2015.

[50] D. Dujic, A. Mester, T. Chaudhuri, A. Coccia, F. Canales, and J. K. Steinke, "Laboratory scale prototype of a power electronic transformer for traction applications," in *Proc. 14th Eur. Conf. Power Electron. Appl.*, 2011, pp. 1–10.

[51] C. Zhao *et al.*, "Design, implementation and performance of a modular power electronic transformer (PET) for railway application," in *Proc. 14th Eur. Conf. Power Electron. Appl.*, 2011, pp. 1–10.

[52] C. Zhao *et al.*, "Power electronic transformer (PET) converter: Design of a 1.2 MW demonstrator for traction applications," in *Proc. Int. Symp. Power Electron. Power Electron., Elect. Drives, Automat. Motion*, 2012, pp. 855–860.

[53] D. Dujic, G. K. Steinke, M. Bellini, M. Rahimo, L. Storasta, and J. K. Steinke, "Characterization of 6.5 kV IGBTs for High-power medium-frequency soft-switched applications," *IEEE Trans. Power Electron.*, vol. 29, no. 2, pp. 906–919, Feb. 2014.

[54] C. Zhao *et al.*, "Power electronic traction transformer—medium voltage prototype," *IEEE Trans. Ind. Electron.*, vol. 61, no. 7, pp. 3257–3268, Jul. 2014.

[55] H. Fan and H. Li, "High-frequency transformer isolated bidirectional DC–DC converter modules with high efficiency over wide load range for 20 kVA solid-state transformer," *IEEE Trans. Power Electron.*, vol. 26, no. 12, pp. 3599–3608, Dec. 2011.

[56] Z. Shu, Z. Kuang, S. Wang, X. Peng, and X. He, "Diode-clamped three-level multi-module cascaded converter based power electronic traction transformer," in *Proc. IEEE 2nd Int. Future Energy Electron. Conf.*, 2015, pp. 1–5.

[57] S. Kouro *et al.*, "Recent advances and industrial applications of multilevel converters," *IEEE Trans. Ind. Electron.*, vol. 57, no. 8, pp. 2553–2580, Aug. 2010.

[58] H. R. Rahnamaee, U. K. Madawala, and D. J. Thrimawithana, "A modified hybrid multi-level converter for high-power high-frequency IPT systems," in *Proc. Int. Power Electron. Appl. Conf. Expo.*, 2014, pp. 624–629.

[59] H. R. Rahnamaee, D. J. Thrimawithana, and U. K. Madawala, "MOSFET based multilevel converter for IPT systems," in *Proc. IEEE Int. Conf. Ind. Technol.*, 2014, pp. 295–300.

[60] H. R. Rahnamaee, U. K. Madawala, and D. J. Thrimawithana, "A multi-level converter for high power-high frequency IPT systems," in *Proc. IEEE 5th Int. Symp. Power Electron. Distrib. Gener. Syst.*, 2014, pp. 1–6.

[61] D. Aggeler, J. Biela, and J. W. Kolar, "A compact, high voltage 25 kW, 50 kHz DC-DC converter based on SiC JFETs," in *Proc. 23rdAnnu. IEEE Appl. Power Electron. Conf. Expo.*, 2008, pp. 801–807.

[62] D. Ronanki, S. A. Singh, and S. S. Williamson, "Comprehensive topological overview of rolling stock architectures and recent trends in electric railway traction systems," *IEEE Trans. Transp. Electrif.*, vol. 3, no. 3, pp. 724–738, Sep. 2017.

[63] W. Platschorre and J. Vangemeren, *Strukton IGBT Inverters and Battery Chargers*. [Online]. Available: https://view.publitas.com/strukton/strukton-power-modules-platform-rolling-stock/page/1

[64] I. Villar, L. Mir, I. Etxeberria-Otadui, J. Colmenero, X. Agirre, and T. Nieva, "Optimal design and experimental validation of a Medium-Frequency 400 kVA power transformer for railway traction applications," in *Proc. IEEE Energy Convers. Congr. Expo.* 2012, pp. 684–690.

[65] L. Lindenmüller, R. Alvarez, P. Kleinichen, and S. Bernet, "Characterization of a 6.5 kV/500 A IGBT module in a series resonant converter," in *Proc. IEEE Energy Convers. Congr. Expo.*, 2011, pp. 4138–4143.

[66] D. Dujic, G. Steinke, E. Bianda, S. Lewdeni-Schmid, C. Zhao, and J. K. Steinke, "Soft switching characterization of a 6.5 kV IGBT for high power LLC resonant DC/DC converter," in *Proc. Int. PCIM Conf.*, 2012, pp. 625–631.

[67] M. Youssef, J. A. A. Qahouq, and M. Orabi, "Analysis and design of LCC resonant inverter for the tranportation systems applications," in *Proc. 25thAnnu. IEEE Appl. Power Electron. Conf. Expo.*, 2010, pp. 1778–1784.
[68] M. Youssef, J. A. A. Qahouq, and M. Orabi, "Electromagnetic compatibility results for an LCC resonant inverter for the tranportation systems," in *Proc. 25th Annu. IEEE Appl. Power Electron. Conf. Expo.*, 2010, pp. 1800–1803.
[69] M. N. Kheraluwala, R. W. Gascoigne, D. M. Divan, and E. D. Baumann, "Performance characterization of a high-power dual active bridge DC-to-DC converter," *IEEE Trans. Ind. Appl.*, vol. 28, no. 6, pp. 1294–1301, Nov./Dec. 1992.
[70] R. Lenke, F. Mura, and R. W. De Doncker, "Comparison of non-resonant and super-resonant dual-active ZVS-operated high-power DC-DC converters," in *Proc.13th Eur. Conf. Power Electron. Appl.*, 2009, pp. 1–10.
[71] W. Mysiński, W. Zając, and T. Płatek, "Resonance converter with a toroidal transformer for a tram-train vehicle," in *Proc. Int. Symp. Power Electron., Elect. Drives, Automat. Motion*, 2014, pp. 1034–1037.
[72] G. D. Demetriades and H. P. Nee, "Characterisation of the soft-switched single-active bridge topology employing a novel control scheme for high-power DC-DC applications," in *Proc. IEEE 36th Power Electron. Spec. Conf.*, 2005, pp. 1947–1951.
[73] H. Reinold, H. Flerlage, G. Hartung, and O. Magin, Medium frequency technology in auxiliary power converter for traction application. 2001. [Online]. Available: https://uic.org/cdrom/2001/wcrr2001/pdf/sp/1_17/224.pdf
[74] A. Garcia-Bediaga, I. Villar, A. Rujas, I. Etxeberria-Otadui, and A. Rufer, "Analytical models of multiphase isolated medium-frequency DC–DC converters," *IEEE Trans. Power Electron.*, vol. 32, no. 4, pp. 2508–2520, Apr. 2017.
[75] B. R. Lin and J. J. Chen, "Zero-voltage-switching/zero-current-switching soft-switching dual-resonant converter," *Int. J. Electron.*, vol. 97, no. 5, pp. 569–585, 2010.
[76] C. E. Kim, K. B. Park, G. W. Moon, and J. Y. Lee, "New multi-output LLC resonant converter for high efficiency and low cost PDP power module," in *Proc.37th IEEE Power Electron. Spec. Conf.*, 2006. pp. 1–7.
[77] K. B. Park, C. E. Kim, G. W. Moon, and M. J. Youn, "New cost-effective PWM single-switch isolated converter," in *Proc. IEEE Power Electron. Spec. Conf.*, 2007, pp. 1715–1720.
[78] T. S. Kim, S. K. Han, G. W. Moon, and M. J. Youn, "High efficiency active clamp forward converter for sustaining power module of plasma display panel," *IEEE Trans. Ind. Electron.*, vol. 55, no. 4, pp. 1874–1876, Apr. 2008.
[79] K. B. Park, C. E. Kim, G. W. Moon, and M. J. Youn, "Voltage oscillation reduction technique for phase-shift full-bridge converter," *IEEE Trans. Ind. Electron.*, vol. 54, no. 5, pp. 2779–2790, Oct. 2007.
[80] H. K. Yoon, E. S. Choi, S. K. Han, G. W. Moon, and M. J. Youn, "Zero-voltage and zero-current switching two-transformer full-bridge converter using the output-voltage-doubler," in *Proc. CES/IEEE 5th Int. Power Electron. Motion Control Conf.*, 2006, pp. 1–5.
[81] J. Liu and N. Zhao, "Improved fault-tolerant method and control strategy based on reverse charging for the power electronic traction transformer," *IEEE Trans. Ind. Electron.*, vol. 65, no. 3, pp. 2672–2682, Mar. 2018.
[82] Q. Fu, J. Zhu, Z. H. Mao, G. Zhang, and T. Chen, "Online condition monitoring of onboard traction transformer core based on core-loss calculation model," *IEEE Trans. Ind. Electron.*, vol. 65, no. 4, pp. 3499–3508, Apr. 2018.
[83] L. H. S. C. Barreto, D. de A. Honório, D. de Souza Oliveira, and P. P. Praça, "An interleaved-stage AC–DC modular cascaded multilevel converter as a solution for MV railway applications," *IEEE Trans. Ind. Electron.*, vol. 65, no. 4, pp. 3008–3016, Apr. 2018.
[84] H. F. Ahmed, H. Cha, A. A. Khan, and H. G. Kim, "A novel buck–boost AC–AC converter with both inverting and noninverting operations and without commutation problem," *IEEE Trans. Power Electron.*, vol. 31, no. 6, pp. 4241–4251, Jun. 2016.
[85] M. Kim, H. Jeong, B. Han, and S. Choi, "New parallel loaded resonant converter with wide output voltage range," *IEEE Trans. Power Electron.*, vol. 33, no. 4, pp. 3106–3114, Apr. 2018.
[86] R. W. Erickson and D. Maksimovic, *Fundamentals of Power Electronics*, 2nd ed. Norwell, MA, USA: Kluwer, 2001.
[87] S. Komeda and H. Fujita, "Power decoupling control method for an isolated single-phase ac-to-dc converter based on high-frequency cycloconverter topology," in *Proc. IEEE 3rd Int. Future Energy Electron. Conf.*, 2017, pp. 1059–1064.
[88] M. Jaritz, T. Rogg, and J. Biela, "Analytical modelling and controller design of a modular series parallel resonant converter system for a solid state 2.88 MW/115-kV long pulse modulator," *IEEE Trans. Power Electron.*, vol. 33, no. 10, pp. 9047–90631, Oct. 2018
[89] J. Huber, G. Ortiz, F. Krismer, N. Widmer, and J. W. Kolar, "η-ρ Pareto optimization of bidirectional half-cycle discontinuous-conduction-mode series-resonant DC/DC converter with fixed voltage transfer ratio," in *Proc. 28th Annu. IEEE Appl. Power Electron. Conf. Expo.* 2013, pp. 1413–1420.
[90] J. E. Huber, J. Miniböck, and J. W. Kolar, "Generic derivation of dynamic model for half-cycle DCM series resonant converters," *IEEE Trans. Power Electron.*, vol. 33, no. 1, pp. 4–7, Jan. 2018.
[91] R. L. Steigerwald, "A comparison of half-bridge resonant converter topologies," *IEEE Trans. Power Electron.*, vol. 3, no. 2, pp. 174–182, Apr. 1988.
[92] M. Jaritz and J. Biela, "Optimal design of a modular series parallel resonant converter for a solid state 2.88 MW/115-kV long pulse modulator," *IEEE Trans. Plasma Sci.*, vol. 42, no. 10, pp. 3014–3022, Oct. 2014.
[93] F. da Silveira Cavalcante and J. W. Kolar, "Design of a 5 kW high output voltage series-parallel resonant DC-DC converter," *Proc. IEEE 34th Annu. Power Electron. Spec. Conf.*, 2003, vol. 4, pp. 1807–1814.
[94] S. D. Johnson, A. F. Witulski, and R. W. Erickson, "Comparison of resonant topologies in high-voltage DC applications," *IEEE Trans. Aerosp. Electron. Syst.*, vol. 24, no. 3, pp. 263–274, May 1988.
[95] Z. Fang, J. Wang, S. Duan, K. Liu, and T. Cai, "Control of an LLC resonant converter using load feedback linearization," *IEEE Trans. Power Electron.*, vol. 33, no. 1, pp. 887–898, Jan. 2018.
[96] M. T. Outeiro, G. Buja, and D. Czarkowski, "Resonant power converters: An overview with multiple elements in the resonant tank network," *IEEE Ind. Electron. Mag.*, vol. 10, no. 2, pp. 21–45, Jun. 2016.

Athanasios Iraklis was born in Thessaloniki (Greece) on May 17, 1989. He received the M.Sc. degree in electrical and computer engineering with specialization in electrical energy systems from the Aristotle University of Thessaloniki, Thessaloniki, Greece, in 2015. He was a Research Engineer with the Energy and Electrical Systems Group, Warwick Manufacturing Group, University of Warwick, Coventry, U.K., and a Research Associate with the Department of Vehicle Energy Concepts, Institute of Vehicle Concepts, German Aerospace Center (DLR), Germany. He is currently a CAE Engineer with AVL Powertrain UK Ltd., Coventry, U.K. His research interests include powertrain modelling and simulation, energy storage, energy management, power electronics, and charging systems for battery-electric vehicles.

Toni Schirmer received the M.Sc. degree in renewable energies from HTW Berlin, Berlin, Germany, in 2014 and the M.Sc. degree in sustainable energy supply from RWTH Aachen, Aachen, Germany in 2017. Since 2017, he has been a Researcher with the Department of Vehicle Energy Concepts, Institute of Vehicle Concepts, DLR, Stuttgart, Germany.

Holger Dittus received the Dipl.-Ing degree in mechanical engineering, from RWTH Aachen, Aachen, Germany, in 2006. From 2006 to 2011, he was a Researcher with the Department of Vehicle Energy Concepts, Institute of Vehicle Concepts, DLR. Since 2011, he has been a Group Leader Energy Management and Verification with the Institute of Vehicle Concepts, DLR, Stuttgart, Germany.

Anna Lusiewicz received the Diploma in theoretical physics from the University of Muenster, Muenster, Germany, in 2013 and is currently working toward the Ph.D. degree in electrical engineering.

She is currently a Research Associate with the Institute of Electrical Energy Conversion, University of Stuttgart, Stuttgart, Germany. Her research interests include dynamic contactless energy transfer on moving objects with a focus on mathematical modeling.

Joachim Winter received the Dipl.-Ing degree in aerospace engineering from Technische Universitt Braunschweig, Braunschweig, Germany, in 1981, and the doctorate in engineering degree from Mercator-Universitt Duisburg, Duisburg, Germany, in 1987. From 1987 to 1990, he was a Development Engineer of flight control with Dornier, Friedrichshafen, Friedrichshafen, Germany. From 1990 to 1994, he was a Referent of control design processes with Dornier, Friedrichshafen. During 1994–1995, he was a Researcher with Daimler-Benz, Stuttgart, Germany. From 1995 to 1998, he was the Head with Future/Pilot Projects, Navigation and Flight Guidance Systems, DASA—NFS, Ulm, Germany. From 1998 to 2000, he was the Manager Marketing & Sales Central Europe, Adtranz (Signal), Braunschweig, Germany. From 1998 to 2004, he was with Manager Systems Engineering and Satellite Navigation Products, Adtranz/Bombardier Transportation (Signal), Braunschweig and Ulm, Germany. From 2004 to 2006, he was the Director, Signaling Technology, Bombardier Transportation (Signal), Stockholm, Sweden. During 2007–2008, he was with the Director Telematics and Site Manager Mannheim, Bombardier Transportation (Signal), Mannheim, Germany. Since 2008, he has been a Senior Researcher of rail vehicles with Institute of Vehicle Concepts, DLR, Stuttgart, Germany, and the Director Telematics with Bombardier Transportation, Montreal, QC, Canada.